ACS OMEGA

Open Access

http://pubs.acs.org/journal/acsodf

Article

Hyaluronic Acid-Targeted Niosomes for Effective Breast Cancer Chemostarvation Therapy

Masoumeh Kaveh Zenjanab, Elaheh Dalir Abdolahinia, Effat Alizadeh, Hamed Hamishehkar, Rasoul Shahbazi, Zahra Ranjbar-Navazi, Rana Jahanban-Esfahlan,* Marziyeh Fathi,* and Seyed Abolghasem Mohammadi*

Cite This: *ACS Omega* 2024, 9, 10875−10885

Read Online

ACCESS | Metrics & More | Article Recommendations

ABSTRACT: Chemotherapy is widely used for cancer therapy; however, its efficacy is limited due to poor targeting specificity and severe side effects. Currently, the next generations of delivery systems with multitasking potential have attracted significant attention for cancer therapy. This study reports on the design and synthesis of a multifunctional nanoplatform based on niosomes (NIO) coloaded with paclitaxel (PTX), a chemotherapeutic drug commonly used to treat breast cancer, and sodium oxamate (SO), a glycolytic inhibitor to enhance the cytotoxicity of anticancer drug, along with quantum dots (QD) as bioimaging agents, and hyaluronic acid (HA) coating for active targeting. HN@QPS nanoparticles with a size of ∼150 nm and a surface charge of −39.9 mV with more than 90% EE for PTX were synthesized. Codelivery of SO with PTX remarkably boosted the anticancer effects of PTX, achieving IC_{50} values of 1−5 and >0.5 ppm for HN@QP and HN@QPS, respectively. Further, HN@QPS treatment enhanced the apoptosis rate by more than 70% in MCF-7 breast cancer cells without significant cytotoxicity on HHF-2 normal cells. Also, quantification of mitochondrial fluorescence showed efficient toxicity against MCF-7 cells. Moreover, the cellular uptake evaluation demonstrated an improved uptake of HN@Q in MCF-7 cells. Taken together, this preliminary research indicated the potential of HN@QPS as an efficient targeted-dual drug delivery nanotheranostic against breast cancer cells.

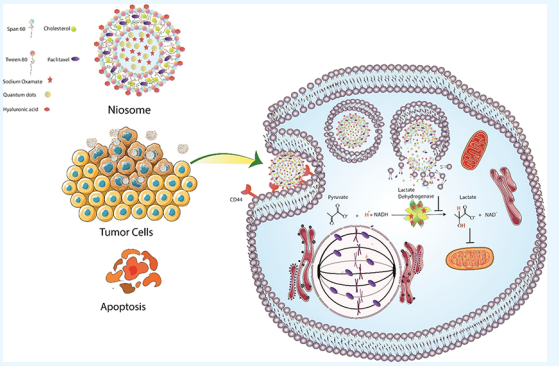

1. INTRODUCTION

Drug protection from degradation by the reticuloendothelial system, enhanced uptake of drugs by target sites, and reduction of unwanted side effects with the aim to improve anticancer efficacy are goals pursued by the design of nanocarriers.[1,2] The stability of nanocarriers such as liposomes and niosomes (NIO) depends on the used lipids (e.g., cholesterol, L-α-soya phosphatidylcholine, etc.) in their structure.[3] These nanovesicles have unique properties including high entrapment efficiency as well as simultaneous delivery of hydrophobic and hydrophilic drugs, which maintain drugs within carriers for a long time, resulting in drug safety and efficacy.[4,5] For the first time, Banghami in 1995 described liposomes as a vesicular drug delivery system (DDS). Then, numerous liposomal vesicles prepared with different phospholipids were employed as drug carriers.[6,7] With all of the merits, liposomes have several disadvantages such as low stability in a variety of pH, toxicity, and high cost. Hence, phospholipids were replaced by nonionic surfactants that realized NIOs as new nanocarriers with unique properties.[8] NIO are prepared by the hydration of nonionic surfactants with a specific ratio of cholesterol. The hydrophilic heads on nonionic surfactants in the structure of NIO have no charge, resulting in safe and nontoxic vesicles.[9] Other properties of NIO that make them distinctive from common nanocarriers are their high physical and chemical stability, size, shape, entrapment, and bioimaging ability, which can be modified by different parameters such as additives, component ratio, or ingredient combination.[10] Studying NIO-containing quantum dots (QD) for targeting cancer cells proved that their combination elevates the therapeutic targets as well as application potential for the imaging of target cancer cells.[11,12] QD are nanoscale semiconductors that can emit glow or fluorescence light when receiving different light sources like a laser.[13,14] QD display excellent properties such as the emission of a broad range of colors based on size from the same materials that are being excited, narrow emission, photobleaching resistance, and great photochemical stability.[15]

Received: December 11, 2023
Revised: January 29, 2024
Accepted: February 6, 2024
Published: February 22, 2024

Paclitaxel (PTX) is one of the major chemotherapy drugs approved in many countries to treat broad-spectrum cancer such as breast cancer.[16] PTX disrupts the dynamics of microtubules by binding to the β subunit of tubulin, disrupts the cytoskeletal structure, and induces cell cycle arrest in the G2 and M phases. PTX is hydrophobic, so to overcome this problem, the use of NIO can aid PTX delivery to the target site.[17,18] In addition, combining PTX with sodium oxamate (SO) can promote the antitumor effects of PTX.[19] As cancer cells predominately use glycolysis to achieve energy, SO inhibits lactate dehydrogenase (LDH) activity, the enzyme that converts lactate to pyruvate, and thus cancer cell growth while enhancing the generation of reactive oxygen species (ROS) in mitochondria, which elevates apoptosis and induces autophagy in cancer cells.[20] It is demonstrated that the release of PTX from pH-sensitive NIO has no significant effects on the HUVEC cells as a normal cell line compared to MCF-7 cancer cells.[21] In addition, the coadministration of PTX with curcumin into the NIO nanoparticles (NPs) improves their synergetic effects and indicates a more toxic effect on MCF-7 cancer cells in comparison to the HHF-2 normal cells.[22] The high expression of $CD44^+$ as an HA receptor on the surface of MCF-7 breast cancer cells can be used for active targeting of nanocarriers by HA coating on the niosome surface.[23,24]

In this study, a new design of NIO was engineered to achieve a multifunctional-targeted theranostic nanosystem. To this end, NIO were coated with an HA shell as a targeting agent, while QD were loaded in their hydrophilic core as imaging moieties. SO and PTX were coencapsulated into NIO NPs to achieve HN@QPS for combination and dual organelle targeting, namely, mitochondria and nucleus by the unique action of SO and PTX. While SO uniquely directs targeting of LDH and mitochondria pathways, PTX inhibits microtubule polymerization and thus induces cell cycle arrest and hamper cell division. Multitasking HN@QPS realizes combination chemostarvation therapy for enhanced and selective killing of MCF-7 breast cancer cells but their nonsignificant effects on HHF-2 normal cells.

2. MATERIALS AND METHODS

2.1. Materials. Span 60, Tween 80, cholesterol, MTT, and 2-(4-amidinophenyl)-6-indolecarbamidine dihydrochloride (DAPI) were purchased from Sigma-Aldrich (St. Louis, MO). PTX was purchased from Sobhan Drugs (Tehran, Iran). All of the solvents (ethanol, methanol, and chloroform) were purchased from Merck Co. (Darmstadt, Germany). The MCF-7 human breast cancer cell line and the HHF-2 cell line were obtained from the National Cell Bank of Iran, Pasteur Institute (Tehran, Iran). RPMI 1640 medium and fetal bovine serum (FBS) were purchased from Gibco, Invitrogen (Paisley, U.K.). An Annexin V-FITC apoptosis detection kit was provided by eBiosciences (MA). The mitochondrial staining kit (ab112145) was supplied by Abcam (Cambridge, U.K.).

2.2. Synthesis of HN@QPS by the Thin-Film Hydration Method. NIO were synthesized by the thin-film hydration method.[8,25] Briefly, Span 60 (8 mg), Tween 80 (18 mg), cholesterol (8 mg), and PTX (2 mg) were dissolved in chloroform and methanol. Then, the solution was put into a round-bottom flask, and a lipid film (proNiosome) was formed after removing the solvent phase in the vacuum by a rotary for 1 h at a 120 rpm rate. The source of InP/ZnS QD was from our previous work.[19] The lipid film was hydrated with 10 mL of PBS containing QD (2 mg), SO (2 mg), and HA (2 mg), and finally, the prepared NIO were sonicated for 7 min to obtain HN@QPS.

2.3. Characterization of HN@QPS. The hydrodynamic diameter (particle size distribution) and surface charge (ζ-potential) were assessed by using dynamic light scattering (DLS) and a Zetasizer Nano ZS (Malvern Instruments Ltd., Malvern, U.K.). The structural analysis of synthesized NPs was carried out by FT-IR measurement (FT-IR Tensor 27 spectrometer). The emission and photoluminescence spectra of QD-loaded NIO were gained by a Cytation 5 cell imaging multimode reader. Also, the morphology of NIO was analyzed by cryogenic transmission electron microscopy (Cryo-TEM).

2.4. Drug Loading Capacity and In Vitro Drug Release Studies. HN@QPS were placed into a dialysis membrane bag (molecular weight cutoff of 12000 Da) and sunk in 50 mL of PBS (pH = 7.4) at 4 °C on a magnetic stirrer for 30 min. Then, the released drug was analyzed with a UV−vis spectrophotometer at 230 nm using a calibration curve. Drug loading (LE) and drug encapsulation (DE) efficiency were calculated using the following formulae.

$$\text{EE}\ (\%) = \frac{\text{initial drug concentration} - \text{unload drug concentration}}{\text{initial drug concentration}} \times 100$$

$$\text{LE}\ (\%) = \frac{\text{amount of drug in carrier (mg/mL)}}{\text{weight of nanoparticle (mg/mL)}} \times 100$$

To study the drug release, the NP suspension was transferred into 50 mL of PBS (pH = 7.4 and 5.8) in a shaker incubator at 37 °C and 80 rpm. At the designated time intervals, 2 mL of the dialysis medium was replaced with 2 mL of fresh PBS (pH = 7.4, 5.8). Then, the release amount of PTX was evaluated by using a UV spectrophotometer at 230 nm. All in vitro release measurements were done in triplicates, and the amount of drug release was estimated by

$$\text{the amount of drug released}\ (\%) = \frac{C_i V_t + \sum_{i=1}^{n} (C_{i-1} V_s)}{m_t} \times 100$$

where m_t is the amount of drug released at time t, V_t is the total volume of the release environment, and V_s is the specified volume removed from the release medium.

2.5. Drug Release Kinetics. The drug kinetic behavior of HN@QP under normal and acidic pH was determined using different mathematical models for drug kinetics, including zero-order, first-order, Higuchi, Hixson−Crowell, and Peppas−Korsmeyer.

2.6. Cytotoxicity Assessment. The MTT assay was used to measure the cytotoxicity and biocompatibility of synthesized NPs. To this, MCF-7 breast cancer cells and HHF-2 fibroblast cells were cultivated at a seeding density of approximately 5.0×10^3 cells per well in a 96-well plate supplemented with RPMI medium with 10% FBS, and then, the cells were incubated at 37 °C and 5% CO_2. After 24 h, the culture medium was removed, and the cells were treated with 200 μL of the medium containing different concentrations of the drug and synthesized NIO. Subsequently, the cells were incubated for 48 and 72 h at 37 °C, and then, 100 μL of MTT solution (1 mg/2 mL in PBS) was added to each well. After 4 h, the MTT solution was removed and replaced with 200 μL of DMSO. The viability of the cells was measured by an ELISA reader at 570 nm absorption wavelength (BioTek Instruments, Winooski).

https://doi.org/10.1021/acsomega.3c09782
ACS Omega 2024, 9, 10875−10885

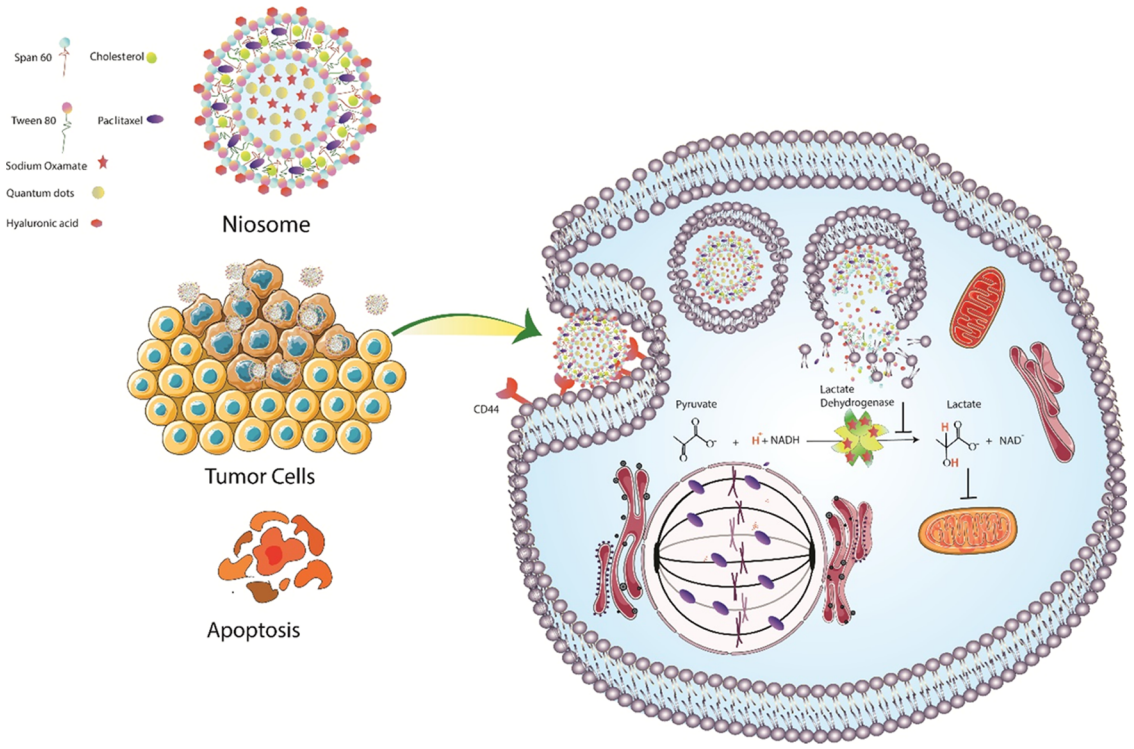

Figure 1. Design concept of multitasking HN@QPS for combination cancer starvation chemotherapy.

2.7. Cellular Uptake. To analyze the cellular uptake of NPs, MCF-7 and HHF-2 cells were seeded at a density of 5.0 × 10^7 cells in six-well plates in the culture medium. After 24 h, the cells were treated with N@Q and HN@Q and incubated at 37 °C for 4 h. Afterward, the cells were washed with PBS, trypsinized, and centrifuged at 160 g for 5 min. Finally, the uptake of NPs was analyzed by FACS Calibur flow cytometry (Becton Dickinson, San Jose, CA).

2.8. Assessment of Apoptosis/Necrosis by Flow Cytometry. To assess the cell apoptosis/necrosis, the MCF-7 breast cancer cells were seeded at a density of 5.0 × 10^7 cells in six-well plates in the culture medium. After 24 h, the medium was removed, and the cells were treated with fresh medium containing the drug and drug-loaded NIO complex and incubated for 72 h. All treated cells were trypsinized, centrifuged at 1000 rpm for 5 min, and washed with 500 μL of PBS. Finally, 100 μL of diluted Annexin V, binding buffer, and PI were added to the cells and incubated in a dark room for 20 min. Then, the samples were centrifuged at 1000 rpm for 5 min, the solution was removed, and 100 μL of binding buffer was added. Finally, the samples were evaluated via the FITC-Annexin V apoptosis detection kit (FACS flow cytometry, BD FACS Calibur, BD Bioscience, CA) to detect the apoptotic cells.

2.9. Mitochondria-Targeting Evaluation. The effect of different nanoformulations as well as free drugs on the mitochondrial activity of MCF-7 cancer cells was studied using a mitochondrial staining kit (Abcam, Cambridge, U.K.). Briefly, the cells were seeded at 5.0 × 10^3 cells per well in a 96-well plate and after 24 h treated with free PTX and different niosome formulations for 72 h. Next, the treated cells were stained with 100 μL of dye-working solution and incubated at 37 °C in a 5% CO_2 incubator for 1 h. Then, the dye-working solution was removed, and PBS buffer and growth medium at a 1:1 concentration were added. Finally, the fluorescence images of stained cells were set to a Cytatio 5 cell imaging multimode reader (Ex/Em = 585/610 nm).

2.10. Statistical Analysis. ANOVA followed by Tukey's post hoc multiple comparison test was used to assess the mean difference among experimental groups. All statistical analyses were performed in triplicates and analyzed by GraphPad Prism software version 9.3. p values < 0.05 were considered statistically significant. ImageJ software was used to quantify the fluorescence intensity.

3. RESULTS AND DISCUSSION

3.1. Characterization of HN@QPS NPs. NIO are self-assembling nonionic vesicles that entrap the hydrophilic drugs into the aqueous core of vesicular particles or adsorb them on the bilayer surfaces, whereas lipophilic drugs are entrapped into the lipophilic domain of NIOs.[4,26] In the current study, to realize a novel targeted theranostic system, HN@QPS was fabricated to target $CD44^+$ on MCF-7 breast cancer, where the QD were used as an imaging agent to monitor cellular uptake, and PTX and SO as therapeutics agents (Figure 1). It is reported that parameters such as cholesterol amount and type of nonionic surfactant significantly affect the size and surface charge of NIOs.[27,28] That is, having high stability and capacity for loading incompatible drugs renders NIO unique NPs for drug delivery purposes. Also, NIO with a hydrophilic headgroup and a hydrophobic tail can entrap the hydrophobic and hydrophilic drugs simultaneously.[29] The size of NPs is one of the important factors in their application because very small or large sizes lead to difficulty in their performance regarding the capability of drug entrapment and drug release behaviors.[30] Besides, the ζ-potential of NPs can indicate the physical stability of NPs in biological situations. It has been reported that ζ-potential values in the range from −30 to +30 mV are usually considered a suitable repulsive force to provide physical stability.[31] As shown in Figure 2a, the size distribution and the

https://doi.org/10.1021/acsomega.3c09782
ACS Omega 2024, 9, 10875−10885

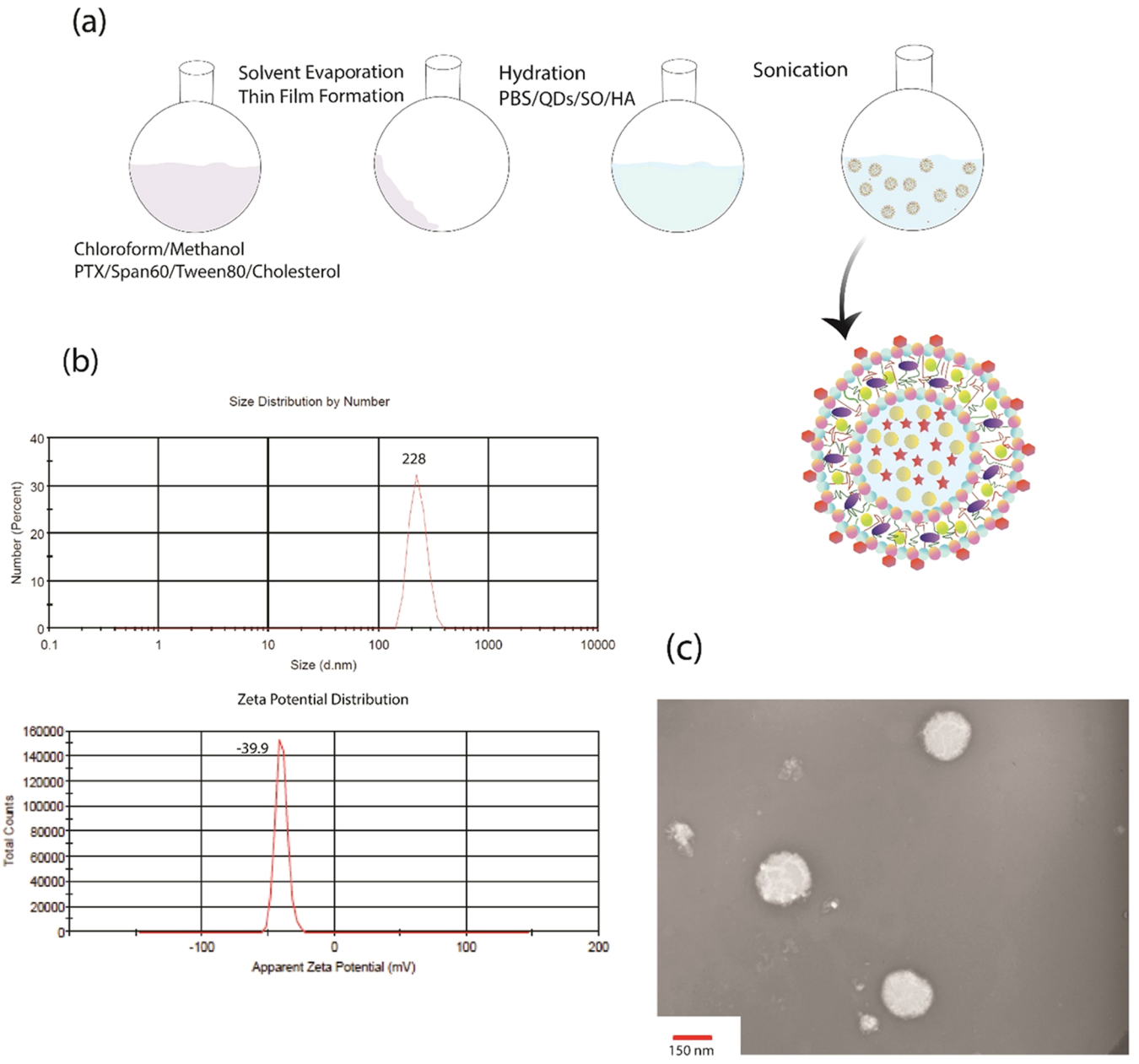

Figure 2. Synthesis process and the DLS analysis of HN@Q (a). Size distribution by number and ζ-potential distribution (b). TEM images of HN@Q for morphological analysis (c).

ζ-potential of HN@QPS were 228 nm and −39.9 mV, respectively. This indicates that HN@QPS has a negative surface charge due to the free carboxylic groups of HA.

TEM analysis showed spherical shapes with a size of around 150 nm for the prepared NPs (Figure 2b). Morphological characterization of NIO obtained by TEM analysis showed less amount than the DLS measurement, as the zetasizer indicates the hydrated diameter form of NPs that is regularly larger than NPs' genuine diameters.[32,33] In general, fenestrations in the spleen can trap the NPs >250 nm, and the liver can accumulate the NPs <70 nm. So, NPs within the range of 70−250 nm are more suitable for drug delivery with high stability in the bloodstream.[34]

The FT-IR spectra were used to determine and analyze the chemical structure of the prepared NPs (Figure 3). The blank NIO structure indicated characteristic peaks at 1738 cm^{-1} attributed to (5-membered ring of cholesterol) groups,[35] 2854 cm^{-1} for C−H symmetric stretch, 1639 cm^{-1} for C−N asymmetric stretching, 1382 cm^{-1} for C−N stretching, and 3417 cm^{-1} as well as 1106 cm^{-1} attributed to the asymmetric stretch of C−O−C groups.[36,37] For N@PTX, the peaks were observed at 1646 cm^{-1} for C═O amide stretching, 1249 cm^{-1} for ester bond stretching, and 951 cm^{-1} for aromatic bonds.[38] N@Q have gained peaks at 1639 cm^{-1} corresponding to the stretching vibration of C−O and 1560 cm^{-1} belonging to the N−H bending of carboxylic groups that confirmed the existence of QD in the NIO compound without chemical interaction.[19] The peak at 2922 cm^{-1} belongs to the alkyl chain that confirms the presence of HA in HN@QP components.[39]

The slight shifts of some peaks in the spectra of HN@Q and HN@QP indicated that NIO has only a physical interaction with other encapsulated moieties. As shown in Figure 4, HN@Q indicated the characteristic photoluminescence emission peak at 450 nm.[33] These data confirm that QD are not

https://doi.org/10.1021/acsomega.3c09782
ACS Omega 2024, 9, 10875−10885

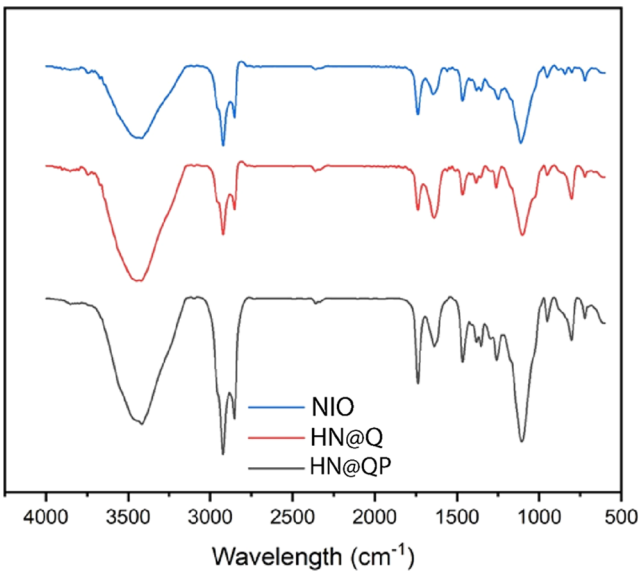

Figure 3. FT-IR spectra of NIO, HN@Q, and HN@QP.

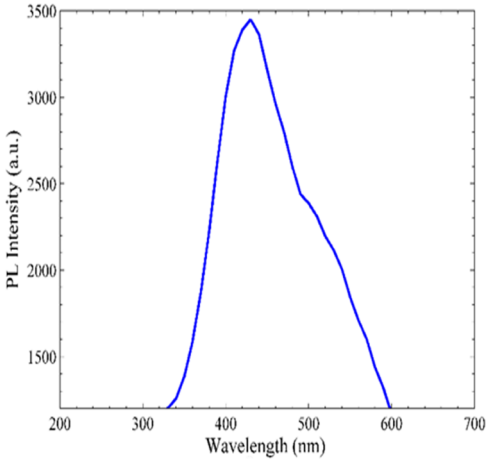

Figure 4. Photoluminescence emission spectra of HN@Q.

quenched during preparation of HN@Q and can be used for cellular bioimaging.

3.2. pH-Responsive Behavior of HN@QP. The balance between the hydrophilic and lipophilic values of a surfactant has a key role in controlling drug loading.[32] The addition of cholesterol causes the formation of vesicles from hydrophobic surfactants, increases their stability, and also improves drug loading.[33] Also, the synthesis of NIO by thin-film hydration methods results in a higher drug-loading content.[40,41]

The %EE values of PTX in N@Q and HN@Q were 98.5 and 93.5%, respectively, indicating the NIO capability in efficient entrapment of the hydrophobic chemotherapeutics. Also, the encapsulation of PTX and SO might occur via a physical interaction between NIO and drugs. As a result, the drug could be protected from hydrolytic or enzymatic degradation; meanwhile, the chemotherapeutic drug's side effects could be minimized. The decrease in %EE of PTX in HN@Q in comparison with N@Q could be due to the steric hindrance. Also, the %LC values of PTX in N@Q and HN@Q were found to be 7.54 and 10.76%, respectively.

Amphiphilic surfactant moieties can promote the drug release and permeation profiles of NIO-based carriers.[28,42,43] The cumulative in vitro release profile of PTX from HN@QP at pH = 7.4 and 5.8 at 37 °C shown in Figure 5 demonstrates a sustained drug release in both pH, with a higher release rate under an acidic environment. Tumor cells have significantly high acidic cytoplasmic pH compared to normal cells. Hence, NPs are more efficient with higher drug release in acidic pH in comparison to physiologic conditions (pH = 7.4).[44] These data demonstrate the pH-sensitive behavior of synthesized multitasking HN@QPS NPs for controlled and selective drug release in the tumor milieu. For the other drug, SO, as there is no specific λmax, the drug release profile is not reported.

3.3. Drug Release Kinetics. The best-fitted model with the highest coefficient of determination (R^2) for release curves at normal and acidic pH for HN@QP was Higuchi's model, indicating that as the diffusion distance increases, drug diffusion occurs at a slower rate (Table 1). Our results are in

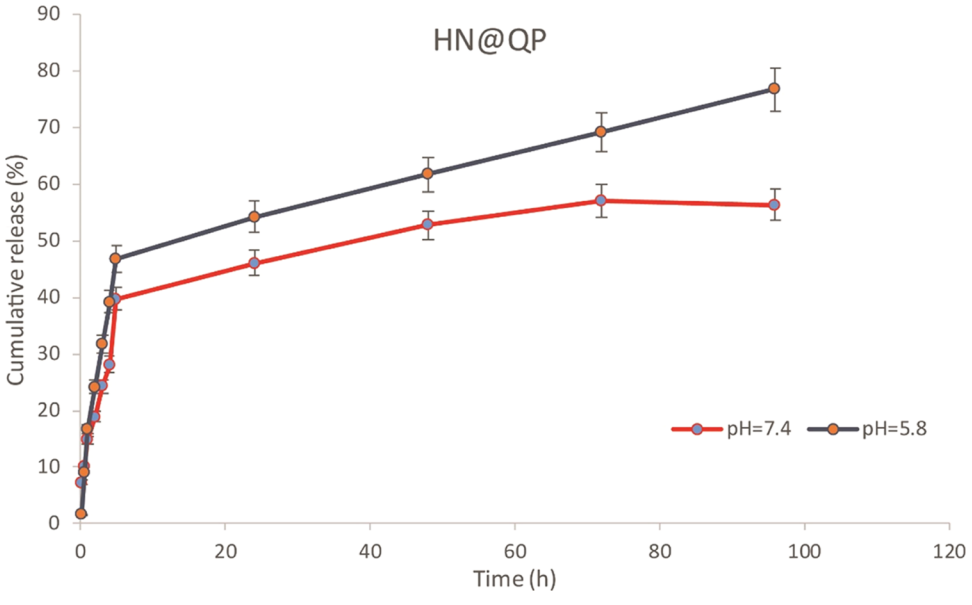

Figure 5. Cumulative in vitro release of PTX from HN@QP NPs.

https://doi.org/10.1021/acsomega.3c09782
ACS Omega 2024, 9, 10875−10885

Table 1. Drug Release Kinetics of HN@QP

		PTX	
kinetic model	equation	pH = 7.4	pH = 5.8
zero order	$F = k_0 t$	R^2 = 0.9172	R^2 = 0.967
first order	$\ln(1 - F) = -k_1 t$	R^2 = 0.9417	R^2 = 0.9856
Higuchi	$F = k_H \sqrt{t}$	**R^2 = 0.9891**	**R^2 = 0.9828**
Hixson−Crowell	$1 - \sqrt[3]{1 - F} = k_{1/3} t$	R^2 = 0.9338	R^2 = 0.9804
Korsmayer−Peppas	$F = k_{k_p} t^n$	R^2 = 0.5749	R^2 = 0.7522

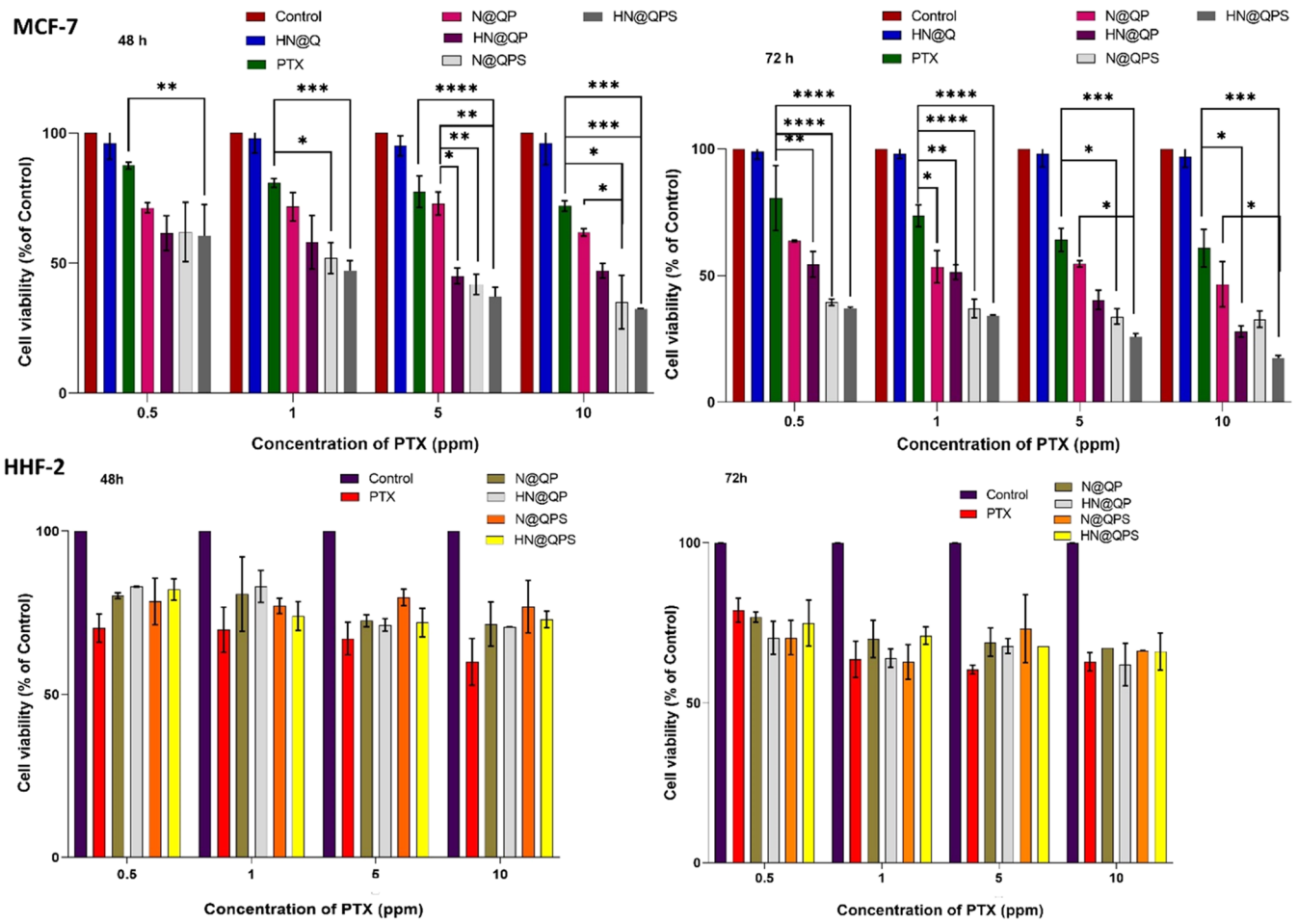

Figure 6. Cytotoxicity of free PTX and niosomal formulations on the MCF-7 and HHF-2 cells after 48 and 72 h. Two-way ANOVA, *, ***, **** represent $p < 0.05$, $p < 0.01$, $p < 0.001$, and $p < 0.0001$, respectively.

line with a previous study that described melatonin release from niosome NPs synthesized by the ball milling method.[45]

3.4. Effect of HN@QPS on Breast Cancer Cell Survival. The cell cytotoxic evaluation of free drug (PTX) and NIO formulations including HN@Q, N@QP, HN@QP, N@QPS, and HN@QPS was assessed by the MTT assay after 48 and 72 h treatments with 0.5, 1, 5, and 10 ppm concentrations of PTX (Figure 6). Our results showed that HN@Q displayed no significant toxicity on MCF-7 cells as well as HHF-2 cells, confirming the biocompatibility of the synthesized NIO-based NPs. Also, the cellular toxicity of HN@QP was significantly higher than the free PTX in all concentrations in a dose- and time-dependent manner. Also, the cytotoxicity on MCF-7 cells showed an increasing trend in the order of N@QP < HN@QP < N@QPS < HN@QPS. The major impact on MCF-7 cells was observed after 72 h of treatment at a concentration of 5 ppm. Meanwhile, niosomal formulations were highly biocompatible, as there was no significant cytotoxicity on the HHF-2 normal cells at studied concentrations. Our results indicated that the combination of PTX with SO boosted the anticancer effects of PTX, as IC_{50} values for HN@QP and HN@QPS for 48 h were determined 1−5 ppm (ppm = μg/mL) and 0.5−1 ppm, respectively. After 72 h of treatment, IC_{50} values for HN@QP and HN@QPS declined to 1−5 and >0.5 ppm, respectively. Thus, SO combination favorably reduces the drug dosing of PTX, potentiating its anticancer response.

3.5. Active Targeting and Targeted Drug Delivery Potential of HN@Q. Active targeting of cancer cells by tumor-specific ligands (such as HA) coated on the NP surface promotes the selective uptake of NPs by target cells through receptor-mediated endocytosis, which increases the intracellular concentration of drugs, as P-glycoprotein cannot

https://doi.org/10.1021/acsomega.3c09782
ACS Omega 2024, 9, 10875−10885

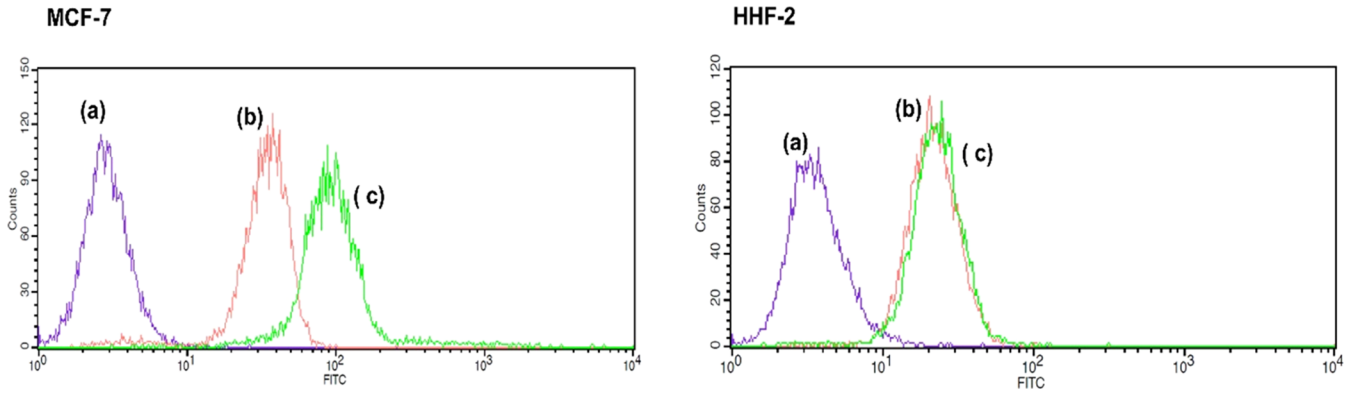

Figure 7. Cellular uptake of NPs. (a) Untreated group, (b) N@Q, and (c) HN@Q.

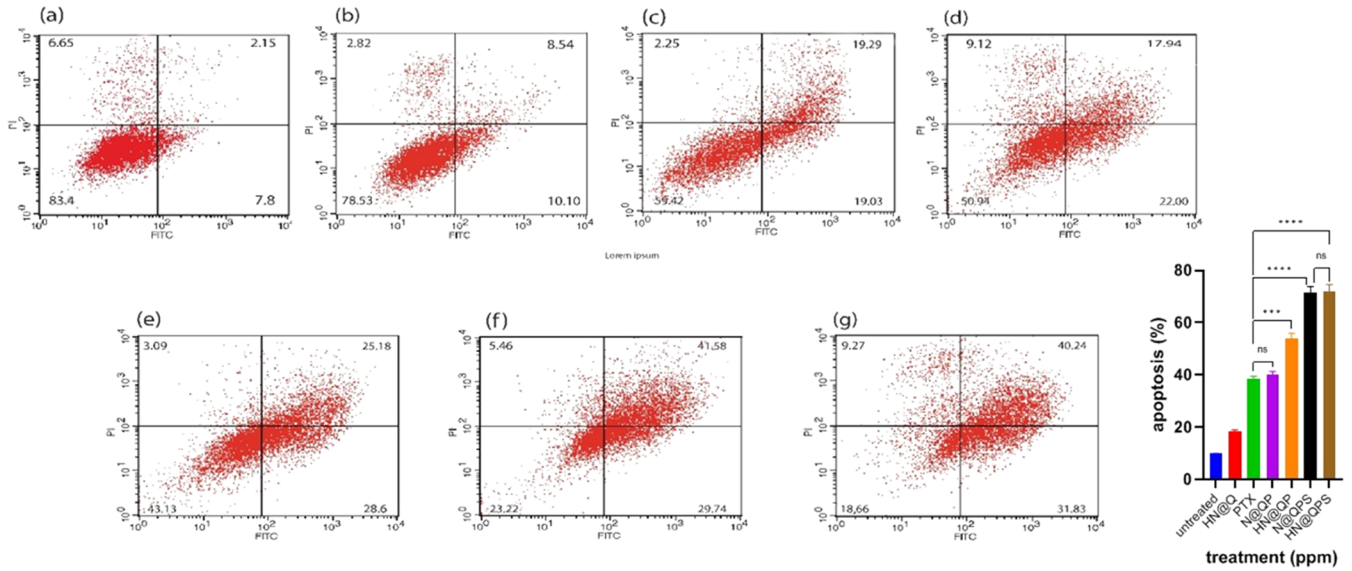

Figure 8. Apoptotic cell death analysis of MCF-7 cells by flow cytometry: (a) untreated group, (b) treated by HN@Q, (c) PTX, (d) N@QP, (e) HN@QP, (f) N@QPS, and (g) HN@QPS. One-way ANOVA, *, **, ***, **** represent $p < 0.05$, $p < 0.01$, $p < 0.001$, and $p < 0.0001$, respectively.

recognize the drugs loaded in NPs to pump them out.[46] Tumor cells have different microenvironments compared with those of normal cells. This difference is related to several aspects such as pH, oxygenation, perfusion, and also metabolic activity.[47] Due to a high rate of angiogenesis, solid tumors display abnormal leaky vasculature with an irregular shape and the lack of a smooth muscle layer. These characteristics can be harnessed to increase NP penetration from the blood circulation to the tumor tissues through enhanced permeability and retention (EPR).[48] Though EPR-mediated passive targeting, which arises from the nanosize scale of NPs, allows them to pass 10−1000 nm pores of endothelial cells, delivery efficiency is barely 0.7−0.0001%;[49,50] thus, the use of active ligand-based targeting is vital to ensure high NP localization and penetration within heterogeneous solid tumor tissue.[51−53]

In our study, not only does HA coating on NIO avoid protein corona formation to enhance the long circulation of NPs, it also promotes active targeting of NPs toward high CD44 expressing MCF-7 breast cancer cells. Plus, this formulation promoted higher cellular uptake of quantum-dot-loaded NPs (HN@Q) and thus compensated for the high negative surface charge of developed niosomes of ∼−30 mV to avoid their electrostatic repulsion by the negatively charged cancer cell membrane.[54] Many studies have indicated that PTX is an antimiotic drug that disrupts cell division to inhibit tumor cell growth.[55] As the main PTX limitation in clinical applications is its low solubility, hopefully, PTX-loaded NIO can overcome this obstacle. Further, to overcome PTX drug resistance, its effects were combined with mitochondria-targeting SO, which significantly improved cell mortality by generation of more reactive oxygen species and cancer cell starvation therapy via targeting glycolysis enzyme, lactate dehydrogenase.[17]

3.6. Cellular Uptake. As mentioned before, NP conjugation with HA can improve the targeting activity by the enhancement of NPaffinity to tumor cells via $CD44^+$ mediated receptors.[56] In this line, the cellular uptake of N@Q and HN@Q was evaluated in the MCF-7 and HHF-2 cells (Figure 7). The results demonstrated the higher cellular uptake efficiency of HA-decorated N@Q compared to N@Q, confirming the HA role in the targeted delivery and its impact on increasing the therapeutic efficiency by possible targeting of CD44, which is a tumor marker of stem cell-like tumor cells (cancer stem cells).[2] Also, cellular uptake analyses of N@Q and HN@Q in HHF-2 as normal cells were similar, which confirmed the

https://doi.org/10.1021/acsomega.3c09782
ACS Omega 2024, 9, 10875−10885

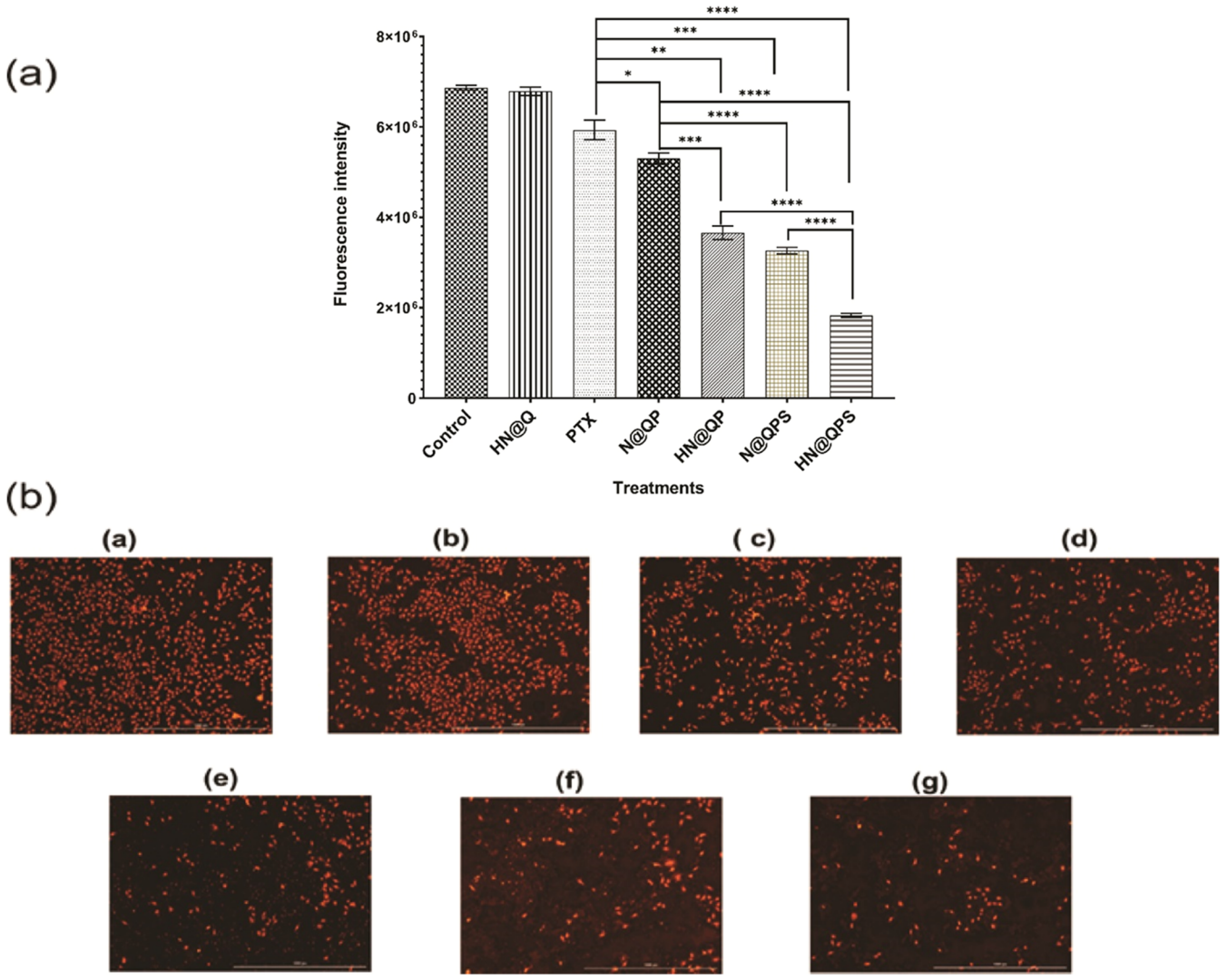

Figure 9. Effect of HN@QPS on mitochondrial integrity. (a) Fluorescence intensity and (b) microscopy images of the (a) untreated group, (b) HN@Q, (c) PTX, (d) N@QP, (e) HN@QP, (f) N@QPS, and (g) HN@QPS. One-way ANOVA, *, **, ***, **** represent $p < 0.05$, $p < 0.01$, $p < 0.001$, and $p < 0.0001$, respectively.

notion that HA coating has no beneficial effects on the uptake of NIO by the HHF-2 cells, which lack the CD44 receptor.

3.7. Effect of HN@QPS on Induction of Apoptotic Death. We next examined the effect of free PTX and HN@QP on MCF-7 cancer cells with a concentration of 5 ppm after 72 h by FITC-labeled Annexin V/PI flow cytometry analysis (Figure 8). The results showed that the apoptosis rates (the late plus early apoptosis) were 9.95, 18.64, 39.32, 39.94, 53.78, 71.32, and 72.07% for untreated control, HN@Q, PTX, N@QP, HN@QP, N@QPS, and HN@QPS, respectively. These results confirmed the enhanced anticancer efficacy of PTX combined with SO and also confirmed the role of HA in increased penetration into cancer cells, which resulted in increased apoptosis of HA-modified niosomes. PTX is shown to induce apoptosis in human lymphoid leukemia cells. It also inhibits the MCF-7 cell proliferation and invasion and increases apoptosis by downregulating the expression of the PI3K/AKT signaling pathway.[57] Mansoori et al. showed that coated liposomes with HA increased the apoptosis in colorectal cancer cells, which overexpressed CD44 and also promoted selective cancer cell mortality.[58] In line with the MTT assay, HN@QPS significantly enhanced induction of apoptosis by more than 70% compared to ∼38% for free PTX and ∼50% for HN@QP, resulting from the combination effect of SO, which inhibits the LDH enzyme, which is key to aerobic glycolysis by cancer cells.[59]

3.8. Mitochondria-Targeting Potential. The potential of HN@QPS to target the mitochondria activity of cancer cells was analyzed using CytoPainter staining for 5 ppm concentration after 72 h of treatment (Figure 9). The quantification trend of mitochondrial fluorescence illustrated the maximum decrease in the mean fluorescence intensity of cells treated with HN@QPS compared to control (∼3.5-fold) and HN@QP (∼2-fold). Our results are in line with a previous study that indicated that the combination of PTX with SO formulated in the MUC1 aptamer-functionalized QD/nano-hydrogel composite resulted in a remarkable reduction in mitochondrial fluorescence compared to MCF-7 cells treated with free PTX.[19] In addition, the combination of SO with other chemotherapy drugs such as doxorubicin has shown synergetic anticancer effects by influencing LDH and disrupting the mitochondria pathways.[60]

https://doi.org/10.1021/acsomega.3c09782
ACS Omega 2024, 9, 10875−10885

4. CONCLUSIONS

Targeted drug delivery systems appear as a promising strategy to increase the effects of conventional chemotherapy drugs on cancer cells via decreasing side effects on normal cells. Multitasking drug carriers with controlled stimuli-responsive drug release, active targeting, and recognizing ability, as well as simultaneous imaging ability, provide ideal nanocarriers for biomedical purposes. The current study attempted to synthesize and characterize NIO with ideal physicochemical properties to achieve an efficient targeted theranostic nanosystem. The modification of NIO by QD and HA realizes a novel nanocarrier that possesses simultaneous imaging, targeting, and dual drug delivery potential. Moreover, designed HN@QPS has a high drug loading capacity for the codelivery of PTX with SO to afford combination effects for enhanced chemostarvation therapy of $CD44^+$ cancer stem cell-like tumors in the absence of off-target effects.

AUTHOR INFORMATION

Corresponding Authors

Rana Jahanban-Esfahlan − *Department of Medical Biotechnology, Faculty of Advanced Medical Sciences, Tabriz University of Medical Sciences, Tabriz 51656-65931, Iran;* orcid.org/0000-0002-5119-252X; Email: jahanbanr@tbzmed.ac.ir

Marziyeh Fathi − *Research Center for Pharmaceutical Nanotechnology, Biomedicine Institute, Tabriz University of Medical Sciences, Tabriz 51656-65931, Iran;* orcid.org/0000-0001-5710-6365; Email: fathi.marziyeh@yahoo.com, fathim@tbzmed.ac.ir

Seyed Abolghasem Mohammadi − *Department of Medical Biotechnology, Faculty of Advanced Medical Sciences, Tabriz University of Medical Sciences, Tabriz 51656-65931, Iran; Department of Plant Breeding and Biotechnology, Faculty of Agriculture, University of Tabriz, Tabriz 51666-16471, Iran;* Email: mohammadi@tabrizu.ac.ir

Authors

Masoumeh Kaveh Zenjanab − *Department of Medical Biotechnology, Faculty of Advanced Medical Sciences, Tabriz University of Medical Sciences, Tabriz 51656-65931, Iran; Research Center for Pharmaceutical Nanotechnology, Biomedicine Institute, Tabriz University of Medical Sciences, Tabriz 51656-65931, Iran*

Elaheh Dalir Abdolahinia − *Research Center for Pharmaceutical Nanotechnology, Biomedicine Institute, Tabriz University of Medical Sciences, Tabriz 51656-65931, Iran; Department of Oral Science and Translation Research, College of Dental Medicine, Nova Southeastern University, Fort Lauderdale, Florida 33314, United States*

Effat Alizadeh − *Department of Medical Biotechnology, Faculty of Advanced Medical Sciences, Tabriz University of Medical Sciences, Tabriz 51656-65931, Iran*

Hamed Hamishehkar − *Drug Applied Research Center, Tabriz University of Medical Sciences, Tabriz 51656-65931, Iran*

Rasoul Shahbazi − *Department of Medical Biotechnology, Faculty of Advanced Medical Sciences, Tabriz University of Medical Sciences, Tabriz 51656-65931, Iran*

Zahra Ranjbar-Navazi − *Research Center for Pharmaceutical Nanotechnology, Biomedicine Institute, Tabriz University of Medical Sciences, Tabriz 51656-65931, Iran*

Complete contact information is available at: https://pubs.acs.org/10.1021/acsomega.3c09782

Author Contributions

M.K.Z.: methodology, investigation, resources, data curation, formal analysis, and writing—original draft preparation. E.D.A.: methodology, investigation, visualization, data curation, and writing—reviewing and editing. E.A.: reviewing and editing. H.H.: methodology, data curation, and reviewing and editing. R.S.: methodology, investigation, and data curation. Z.R.-N.: methodology and investigation. R.J.-E.: critical paper editing for intellectual content. M.F.: supervision, conceptualization, visualization, data curation, validation, and writing—reviewing and editing. S.A.M.: supervision and writing—reviewing and editing.

Funding

This study is a part of an M.Sc. thesis supported by the financial support provided by Tabriz University of Medical Sciences (Grant No. 67477).

Notes

The authors declare no competing financial interest.

ACKNOWLEDGMENTS

The authors want to thank Dr. Parvin Samadi Pakchin for providing constructive guidance for data representation, the Research Center for Pharmaceutical Nanotechnology, and Department of Medical Biotechnology, Faculty of Advanced Medical Sciences, Tabriz University of Medical Sciences, Tabriz, Iran.

REFERENCES

(1) Baghban, R.; Roshangar, L.; Jahanban-Esfahlan, R.; Seidi, K.; Ebrahimi-Kalan, A.; Jaymand, M.; Kolahian, S.; Javaheri, T.; Zare, P. Tumor microenvironment complexity and therapeutic implications at a glance. *Cell Commun. Signaling* **2020**, *18* (1), 59.

(2) Doustmihan, A.; Fathi, M.; Mazloomi, M.; Salemi, A.; Hamblin, M. R.; Jahanban-Esfahlan, R. Molecular targets, therapeutic agents and multitasking nanoparticles to deal with cancer stem cells: A narrative review. *J. Controlled Release* **2023**, *363*, 57−83.

(3) Dianat-Moghadam, H.; Heydarifard, M.; Jahanban-Esfahlan, R.; Panahi, Y.; Hamishehkar, H.; Pouremamali, F.; Rahbarghazi, R.; Nouri, M. Cancer stem cells-emanated therapy resistance: Implications for liposomal drug delivery systems. *J. Controlled Release* **2018**, *288*, 62−83.

(4) Moghassemi, S.; Hadjizadeh, A. Nano-niosomes as nanoscale drug delivery systems: an illustrated review. *J. Controlled Release* **2014**, *185*, 22−36.

(5) Marianecci, C.; Di Marzio, L.; Rinaldi, F.; Celia, C.; Paolino, D.; Alhaique, F.; Esposito, S.; Carafa, M. Niosomes from 80s to present: the state of the art. *Adv. Colloid Interface Sci.* **2014**, *205*, 187−206.

(6) Al-Jamal, W. T.; Kostarelos, K. Liposomes: from a clinically established drug delivery system to a nanoparticle platform for theranostic nanomedicine. *Acc. Chem. Res.* **2011**, *44* (10), 1094−1104.

(7) Guimarães, D.; Cavaco-Paulo, A.; Nogueira, E. Design of liposomes as drug delivery system for therapeutic applications. *Int. J. Pharm.* **2021**, *601*, No. 120571.

(8) Uchegbu, I. F.; Vyas, S. P. Non-ionic surfactant based vesicles (niosomes) in drug delivery. *Int. J. Pharm.* **1998**, *172* (1−2), 33−70.

(9) Bhardwaj, P.; Tripathi, P.; Gupta, R.; Pandey, S. Niosomes: A review on niosomal research in the last decade. *J. Drug Delivery Sci. Technol.* **2020**, *56*, No. 101581.

(10) Makeshwar, K. B.; Wasankar, S. R. Niosome: a novel drug delivery system. *Asian J. Pharm. Res.* **2013**, *3* (1), 16−20.

(11) Ag Seleci, D.; Maurer, V.; Barlas, F. B.; Porsiel, J. C.; Temel, B.; Ceylan, E.; Timur, S.; Stahl, F.; Scheper, T.; Garnweitner, G.

Transferrin-decorated niosomes with integrated InP/ZnS quantum dots and magnetic iron oxide nanoparticles: dual targeting and imaging of glioma. *Int. J. Mol. Sci.* **2021**, *22* (9), 4556.
(12) Nowroozi, F.; Dadashzadeh, S.; Soleimanjahi, H.; Haeri, A.; Shahhosseini, S.; Javidi, J.; Karimi, H. Theranostic niosomes for direct intratumoral injection: marked enhancement in tumor retention and anticancer efficacy. *Nanomedicine* **2018**, *13* (17), 2201−2219.
(13) Dey, N. S.; Rao, M. B. Quantum dot: Novel carrier for drug delivery. *Int. J. Res. Pharm. Biomed. Sci.* **2011**, *2* (2), 448−458.
(14) Alivisatos, A. P. Semiconductor clusters, nanocrystals, and quantum dots. *Science* **1996**, *271* (5251), 933−937.
(15) Cui, L.; Li, C.-c.; Tang, B.; Zhang, C.-y. Advances in the integration of quantum dots with various nanomaterials for biomedical and environmental applications. *Analyst* **2018**, *143* (11), 2469−2478.
(16) Markman, M.; Mekhail, T. M. Paclitaxel in cancer therapy. *Expert Opin. Pharmacother.* **2002**, *3* (6), 755−766.
(17) Weaver, B. A. How Taxol/paclitaxel kills cancer cells. *Mol. Biol. Cell* **2014**, *25* (18), 2677−2681.
(18) Bayindir, Z. S.; Beşikci, A.; Yüksel, N. Paclitaxel-loaded niosomes for intravenous administration: pharmacokineticsand tissue distribution in rats. *Turk. J. Med. Sci.* **2015**, *45* (6), 1403−1412.
(19) Ranjbar-Navazi, Z.; Fathi, M.; Abdolahinia, E. D.; Omidi, Y.; Davaran, S. MUC-1 aptamer conjugated InP/ZnS quantum dots/nanohydrogel fluorescent composite for mitochondria-mediated apoptosis in MCF-7 cells. *Mater. Sci. Eng. C* **2021**, *118*, No. 111469.
(20) Zhao, Z.; Han, F.; Yang, S.; Wu, J.; Zhan, W. Oxamate-mediated inhibition of lactate dehydrogenase induces protective autophagy in gastric cancer cells: Involvement of the Akt−mTOR signaling pathway. *Cancer Lett.* **2015**, *358* (1), 17−26.
(21) Barani, M.; Hajinezhad, M. R.; Sargazi, S.; Rahdar, A.; Shahraki, S.; Lohrasbi-Nejad, A.; Baino, F. In vitro and in vivo anticancer effect of pH-responsive paclitaxel-loaded niosomes. *J. Mater. Sci.: Mater. Med.* **2021**, *32* (12), 147.
(22) Alemi, A.; Zavar Reza, J.; Haghiralsadat, F.; Zarei Jaliani, H.; Haghi Karamallah, M.; Hosseini, S. A.; Haghi Karamallah, S. Paclitaxel and curcumin coadministration in novel cationic PEGylated niosomal formulations exhibit enhanced synergistic antitumor efficacy. *J. Nanobiotechnol.* **2018**, *16* (1), 28.
(23) Fang, X. J.; Jiang, H.; Zhao, X. P.; Jiang, W. M. The role of a new CD44st in increasing the invasion capability of the human breast cancer cell line MCF-7. *BMC Cancer* **2011**, *11* (1), 290.
(24) Wichayapreechar, P.; Anuchapreeda, S.; Phongpradist, R.; Rungseevijitprapa, W.; Ampasavate, C. Dermal targeting of Centella asiatica extract using hyaluronic acid surface modified niosomes. *J. Liposome Res.* **2020**, *30* (2), 197−207.
(25) Alemi, A.; Farrokhifar, M.; Zare-Zardini, H.; Karamallah, M. H. A Comparison between the Anticancer Activities of Free Paclitaxel and Paclitaxel-Loaded Niosome Nanoparticles on Human Acute Lymphoblastic Leukemia Cell Line Nalm-6. *Iran. J. Pediatr. Hematol. Oncol.* **2018**, *8* (3), 153−160.
(26) Pardakhty, A.; Moazeni, E. Nano-niosomes in drug, vaccine and gene delivery: a rapid overview. *Nanomed. J.* **2013**, *1* (1), 1−12.
(27) Suriyaprakash, T. N. K.; Parthiban, S.; Prabu, S. L.; Sumathi, A. Formulation and evaluation of paclitaxel niosome for its improved anti-cancer activity. *Acta Pharm. Sci.* **2011**, *53* (3), 469−475.
(28) Khan, M. I.; Madni, A.; Peltonen, L. Development and in-vitro characterization of sorbitan monolaurate and poloxamer 184 based niosomes for oral delivery of diacerein. *Eur. J. Pharm. Sci.* **2016**, *95*, 88−95.
(29) Gharbavi, M.; Amani, J.; Kheiri-Manjili, H.; Danafar, H.; Sharafi, A. Niosome: a promising nanocarrier for natural drug delivery through blood-brain barrier. *Adv. Pharmacol. Sci.* **2018**, *2018*, No. 6847971.
(30) Umbarkar, M. G. Niosome as a novel pharmaceutical drug delivery: a brief review highlighting formulation, types, composition and application. *Indian J. Pharm. Educ. Res.* **2021**, *55* (1), 34.
(31) Amiryaghoubi, N.; Abdolahinia, E. D.; Nakhlband, A.; Aslzad, S.; Fathi, M.; Barar, J.; Omidi, Y. Smart chitosan−folate hybrid magnetic nanoparticles for targeted delivery of doxorubicin to osteosarcoma cells. *Colloids Surf., B* **2022**, *220*, No. 112911.
(32) Kumar, G. P.; Rajeshwarrao, P. Nonionic surfactant vesicular systems for effective drug delivery—an overview. *Acta Pharm. Sin. B* **2011**, *1* (4), 208−219.
(33) Lawrence, M.; Chauhan, S.; Lawrence, S.; Barlow, D. The formation, characterization and stability of non-ionic surfactant vesicles. *STP Pharma Sci.* **1996**, *6* (1), 49−60.
(34) Barar, J.; Omidi, Y. Surface modified multifunctional nanomedicines for simultaneous imaging and therapy of cancer. *BioImpacts* **2014**, *4* (1), 3.
(35) Khan, M. I.; Madni, A.; Ahmad, S.; Khan, A.; Rehmanand, M.; Mahmood, M. A. ATR-FTIR Based Pre and Post Formulation Compatibility Studies for the Design of Niosomal Drug Delivery System Containing Nonionic Amphiphiles and Chondroprotective Drug. *J. Chem. Soc. Pak.* **2015**, *37* (3), 527−534.
(36) Mehta, S.; Jindal, N. Formulation of Tyloxapol niosomes for encapsulation, stabilization and dissolution of anti-tubercular drugs. *Colloids Surf., B* **2013**, *101*, 434−441.
(37) Samed, N.; Sharma, V.; Sundaramurthy, A. Hydrogen bonded niosomes for encapsulation and release of hydrophilic and hydrophobic anti-diabetic drugs: an efficient system for oral anti-diabetic formulation. *Appl. Surf. Sci.* **2018**, *449*, 567−573.
(38) Xie, Y.; Yao, Y. Incorporation with dendrimer-like biopolymer leads to improved soluble amount and in vitro anticancer efficacy of paclitaxel. *J. Pharm. Sci.* **2019**, *108* (6), 1984−1990.
(39) Al-Sibani, M.; Al-Harrasi, A.; Neubert, R. Characterization of linear and chemically cross-linked hyaluronic acid using various analytical techniques including FTIR, ESI-MS, H1 NMR, and SEM. *J. Biochem. Anal. Stud.* **2018**, *3*, 1−8.
(40) Jadon, P. S.; Gajbhiye, V.; Jadon, R. S.; Gajbhiye, K. R.; Ganesh, N. Enhanced oral bioavailability of griseofulvin via niosomes. *AAPS PharmSciTech* **2009**, *10*, 1186−1192.
(41) Barani, M.; Hajinezhad, M. R.; Sargazi, S.; Rahdar, A.; Shahraki, S.; Lohrasbi-Nejad, A.; Baino, F. In vitro and in vivo anticancer effect of pH-responsive paclitaxel-loaded niosomes. *J. Mater. Sci.: Mater. Med.* **2021**, *32*, 147.
(42) Kamel, R.; Basha, M.; Abd El-Alim, S. H. Development of a novel vesicular system using a binary mixture of sorbitan monostearate and polyethylene glycol fatty acid esters for rectal delivery of rutin. *J. Liposome Res.* **2013**, *23* (1), 28−36.
(43) Shi, Z.; Chen, J.; Yin, X. Effect of anionic−nonionic-mixed surfactant micelles on solubilization of PAHs. *J. Air Waste Manage. Assoc.* **2013**, *63* (6), 694−701.
(44) Lee, E. S.; Na, K.; Bae, Y. H. Doxorubicin loaded pH-sensitive polymeric micelles for reversal of resistant MCF-7 tumor. *J. Controlled Release* **2005**, *103* (2), 405−418.
(45) Temprom, L.; Krongsuk, S.; Thapphasaraphong, S.; Priperm, A.; Namuangruk, S. A novel preparation and characterization of melatonin loaded niosomes based on using a ball milling method. *Mater. Today Commun.* **2022**, *31*, No. 103340.
(46) Wang, J.; Wang, F.; Li, F.; Zhang, W.; Shen, Y.; Zhou, D.; Guo, S. A multifunctional poly (curcumin) nanomedicine for dual-modal targeted delivery, intracellular responsive release, dual-drug treatment and imaging of multidrug resistant cancer cells. *J. Mater. Chem. B* **2016**, *4* (17), 2954−2962.
(47) Jahanban-Esfahlan, R.; Seidi, K.; Banimohamad-Shotorbani, B.; Jahanban-Esfahlan, A.; Yousefi, B. Combination of nanotechnology with vascular targeting agents for effective cancer therapy. *J. Cell. Physiol.* **2018**, *233* (4), 2982−2992.
(48) Jahanban-Esfahlan, R.; de la Guardia, M.; Ahmadi, D.; Yousefi, B. Modulating tumor hypoxia by nanomedicine for effective cancer therapy. *J. Cell. Physiol.* **2018**, *233* (3), 2019−2031.
(49) Poon, W.; Kingston, B. R.; Ouyang, B.; Ngo, W.; Chan, W. C. W. A framework for designing delivery systems. *Nat. Nanotechnol.* **2020**, *15* (10), 819−829.
(50) Cheng, Y.-H.; He, C.; Riviere, J. E.; Monteiro-Riviere, N. A.; Lin, Z. Meta-Analysis of Nanoparticle Delivery to Tumors Using a

https://doi.org/10.1021/acsomega.3c09782
ACS Omega 2024, 9, 10875−10885

Physiologically Based Pharmacokinetic Modeling and Simulation Approach. *ACS Nano* **2020**, *14* (3), 3075−3095.
(51) Jahanban-Esfahlan, R.; Seidi, K.; Monhemi, H.; Adli, A. D. F.; Minofar, B.; Zare, P.; Farajzadeh, D.; Farajnia, S.; Behzadi, R.; Abbasi, M. M.; Zarghami, N.; Javaheri, T. RGD delivery of truncated coagulase to tumor vasculature affords local thrombotic activity to induce infarction of tumors in mice. *Sci. Rep.* **2017**, *7* (1), No. 8126.
(52) Seidi, K.; Jahanban-Esfahlan, R.; Zarghami, N. Tumor rim cells: From resistance to vascular targeting agents to complete tumor ablation. *Tumour Biol.* **2017**, *39* (3), No. e01.
(53) Shi, Y.; van der Meel, R.; Chen, X.; Lammers, T. The EPR effect and beyond: Strategies to improve tumor targeting and cancer nanomedicine treatment efficacy. *Theranostics* **2020**, *10* (17), 7921−7924.
(54) Azizi, M.; Jahanban-Esfahlan, R.; Samadian, H.; Hamidi, M.; Seidi, K.; Dolatshahi-Pirouz, A.; Yazdi, A. A.; Shavandi, A.; Laurent, S.; Be Omide Hagh, M.; Kasaiyan, N.; Santos, H. A.; Shahbazi, M.-A. Multifunctional nanostructures: Intelligent design to overcome biological barriers. *Mater. Today Bio* **2023**, *20*, No. 100672.
(55) Abu Samaan, T. M.; Samec, M.; Liskova, A.; Kubatka, P.; Büsselberg, D. Paclitaxel's mechanistic and clinical effects on breast cancer. *Biomolecules* **2019**, *9* (12), 789.
(56) Kim, J. H.; Moon, M. J.; Kim, D. Y.; Heo, S. H.; Jeong, Y. Y. Hyaluronic acid-based nanomaterials for cancer therapy. *Polymers* **2018**, *10* (10), 1133.
(57) Wang, T. H.; Wang, H. S.; Soong, Y. K. Paclitaxel-induced cell death: where the cell cycle and apoptosis come together. *Cancer* **2000**, *88* (11), 2619−2628.
(58) Mansoori, B.; Mohammadi, A.; Abedi-Gaballu, F.; Abbaspour, S.; Ghasabi, M.; Yekta, R.; Shirjang, S.; Dehghan, G.; Hamblin, M. R.; Baradaran, B. Hyaluronic acid-decorated liposomal nanoparticles for targeted delivery of 5-fluorouracil into HT-29 colorectal cancer cells. *J. Cell. Physiol.* **2020**, *235* (10), 6817−6830.
(59) Valvona, C. J.; Fillmore, H. L. Oxamate, but not selective targeting of LDH-A, inhibits medulloblastoma cell glycolysis, growth and motility. *Brain Sci.* **2018**, *8* (4), 56.
(60) Coronel-Hernández, J.; Salgado-García, R.; León, C.-D.; Jacobo-Herrera, N.; Millan-Catalan, O.; Delgado-Waldo, I.; Campos-Parra, A. D.; Rodríguez-Morales, M.; Delgado-Buenrostro, N. L.; Pérez-Plasencia, C. Combination of Metformin, Sodium Oxamate and Doxorubicin Induces Apoptosis and Autophagy in Colorectal Cancer Cells via Downregulation HIF-1α. *Front. Oncol.* **2021**, *11*, No. 594200.

https://doi.org/10.1021/acsomega.3c09782
ACS Omega 2024, 9, 10875−10885